Received: 4 September 2018 | Revised: 16 February 2019 | Accepted: 20 February 2019

DOI: 10.1111/bph.14671

RESEARCH PAPER

VU0810464, a non-urea G protein-gated inwardly rectifying K^+ ($K_{ir}3$/GIRK) channel activator, exhibits enhanced selectivity for neuronal $K_{ir}3$ channels and reduces stress-induced hyperthermia in mice

Baovi N. Vo[1] | Kristopher K. Abney[2] | Allison Anderson[1] | Ezequiel Marron Fernandez de Velasco[1] | Michael A. Benneyworth[3] | John Scott Daniels[4] | Ryan D. Morrison[4] | Corey R. Hopkins[5] | Charles David Weaver[6] | Kevin Wickman[1]

[1] Department of Pharmacology, University of Minnesota, Minneapolis, MN

[2] School of Graduate Studies and Research, Meharry Medical College, Nashville, TN

[3] Department of Neuroscience, University of Minnesota, Minneapolis, MN

[4] Research and Development, Precera Bioscience, Inc., Franklin, TN

[5] Department of Pharmaceutical Sciences, College of Pharmacy, University of Nebraska Medical Center, Omaha, NE

[6] Departments of Pharmacology and Chemistry, Vanderbilt University, Nashville, TN

Correspondence
Kevin Wickman, Department of Pharmacology, University of Minnesota, 6-120 Jackson Hall, 321 Church Street SE, Minneapolis, MN 55455.
Email: wickm002@umn.edu

Funding information
National Heart, Lung, and Blood Institute, Grant/Award Numbers: HL105550 and HL139090; National Institute of Mental Health, Grant/Award Number: MH107399; National Institute on Drug Abuse, Grant/Award Number: DA034696; Biomedical Research Support Shared Instrumentation, Grant/Award Number: S10

Background and Purpose: G protein-gated inwardly rectifying K^+ ($K_{ir}3$) channels moderate the activity of excitable cells and have been implicated in neurological disorders and cardiac arrhythmias. Most neuronal $K_{ir}3$ channels consist of $K_{ir}3.1$ and $K_{ir}3.2$ subtypes, while cardiac $K_{ir}3$ channels consist of $K_{ir}3.1$ and $K_{ir}3.4$ subtypes. Previously, we identified a family of urea-containing $K_{ir}3$ channel activators, but these molecules exhibit suboptimal pharmacokinetic properties and modest selectivity for $K_{ir}3.1/3.2$ relative to $K_{ir}3.1/3.4$ channels. Here, we characterize a non-urea activator, VU0810464, which displays nanomolar potency as a $K_{ir}3.1/3.2$ activator, improved selectivity for neuronal $K_{ir}3$ channels, and improved brain penetration.

Experimental Approach: We used whole-cell electrophysiology to measure the efficacy and potency of VU0810464 in neurons and the selectivity of VU0810464 for neuronal and cardiac $K_{ir}3$ channel subtypes. We tested VU0810464 in vivo in stress-induced hyperthermia and elevated plus maze paradigms. Parallel studies with ML297, the prototypical activator of $K_{ir}3.1$-containing $K_{ir}3$ channels, were performed to permit direct comparisons.

Key Results: VU0810464 and ML297 exhibited comparable efficacy and potency as neuronal $K_{ir}3$ channel activators, but VU0810464 was more selective for neuronal $K_{ir}3$ channels. VU0810464, like ML297, reduced stress-induced hyperthermia in a $K_{ir}3$-dependent manner in mice. ML297, but not VU0810464, decreased anxiety-related behaviour as assessed with the elevated plus maze test.

Conclusion and Implications: VU0810464 represents a new class of $K_{ir}3$ channel activator with enhanced selectivity for $K_{ir}3.1/3.2$ channels. VU0810464 may be useful for examining $K_{ir}3.1/3.2$ channel contributions to complex behaviours and for probing the potential of $K_{ir}3$ channel-dependent manipulations to treat neurological disorders.

Abbreviations: EPM, elevated plus maze; HPC, hippocampal; $K_{ir}3$, G protein-gated inwardly rectifying potassium; SAN, sino-atrial nodal; SIH, stress-induced hyperthermia; Tl^+, thallium; VU0810464, C(18)-H(21)-N(3)-O-F-Cl

1 | INTRODUCTION

G protein-gated inwardly rectifying K^+ ($K_{ir}3$, also known as GIRK) channels are activated upon stimulation of receptors coupled to inhibitory ($G_{i/o}$) G proteins, leading to cell hyperpolarization (Slesinger & Wickman, 2015). $K_{ir}3$ channels are critical regulators of neuronal excitability (Lujan, Marron Fernandez de Velasco, Aguado, & Wickman, 2014). Dysregulation of $K_{ir}3$ channel activity has been associated with several neurological disorders such as autism, schizophrenia, epilepsy, Down syndrome, Alzheimer's disease, addiction, mood-related disorders, and pain (Berg, Alaburda, & Hounsgaard, 2007; Brewer & Baccei, 2018; Crabtree et al., 2017; Nimitvilai, Lopez, & Woodward, 2018; Sanchez-Rodriguez et al., 2017; Selimbeyoglu et al., 2017; Usowicz & Garden, 2012; Vogels, Sprekeler, Zenke, Clopath, & Gerstner, 2011; Walsh, 2011).

$K_{ir}3$ channels are homo or heterotetrameric complexes, formed by various combinations of four subunits ($K_{ir}3.1$–3.4; Lujan et al., 2014). The prototypical neuronal $K_{ir}3$ channel consists of **$K_{ir}3.1$** and **$K_{ir}3.2$** channels (Lujan et al., 2014). Indeed, genetic ablation of either *Kcnj3* (*Girk1*) or *Kcnj6* (*Girk2*) in mice yields a complete loss or significant reduction in $K_{ir}3$-dependent signalling in most neuron populations evaluated to date (Lujan et al., 2014). $K_{ir}3$ channels are also present in the heart (Lee et al., 2018; Mesirca et al., 2013; Wydeven, Posokhova, Xia, Martemyanov, & Wickman, 2014). Cardiac $K_{ir}3$ channels, consisting primarily of $K_{ir}3.1$ and **$K_{ir}3.4$** channels, are critical mediators of parasympathetic effects on heart rate and rhythm (Lee et al., 2018; Mesirca et al., 2016; Mesirca et al., 2013; Wickman, Nemec, Gendler, & Clapham, 1998; Wydeven, Posokhova, et al., 2014).

While specific $K_{ir}3$ channel subtypes make discrete contributions to organ physiology and behaviour, the lack of subtype-selective $K_{ir}3$ channel activators with pharmacodynamic and pharmacokinetic properties suitable for in vivo testing has limited rigorous evaluation of the physiological significance and therapeutic potential of $K_{ir}3$ channel activation. A high-throughput screen led to the development of **ML297**, a potent small molecule activator of $K_{ir}3$ channels (Kaufmann et al., 2013). ML297 selectively activates $K_{ir}3.1$ channels and shows a weak preference for $K_{ir}3.1/3.2$ (neuronal) over $K_{ir}3.1/3.4$ (cardiac) channel subtypes (Kaufmann et al., 2013). ML297 exhibits antiepileptic and $K_{ir}3$-dependent anxiolytic efficacy in mice at doses that have no evident impact on motor activity or addiction-related behaviour (Huang et al., 2018; Kaufmann et al., 2013; Wydeven, Marron Fernandez de Velasco, et al., 2014).

ML297 contains a phenyl moiety and a pyrazole linked by a urea (Kaufmann et al., 2013). The utility of urea-containing compounds is limited due to significant pharmacokinetic liabilities including poor solubility, low brain penetration, and modest selectivity for the $K_{ir}3.1/3.2$ channel subtype (Kaufmann et al., 2013). An amide-bridged $K_{ir}3$ channel activator scaffold has also been investigated, but this scaffold has failed to yield compounds that prefer $K_{ir}3.1/3.2$ over $K_{ir}3.1/3.4$ channel subtypes (Ramos-Hunter et al., 2013). Furthermore, the compounds from this scaffold were lower in potency than ML297.

What is already known

- G protein-gated inwardly rectifying K^+ ($K_{ir}3$) channels of distinct subtypes regulate the excitability of neurons and cardiomyocytes.
- Current $K_{ir}3$ channel modulators have suboptimal pharmacokinetic properties and relatively poor selectivity for neuronal $K_{ir}3$ channels.

What this study adds

- The novel $K_{ir}3$ channel activator, VU0810464, exhibits enhanced selectivity for neuronal $K_{ir}3$ channels.
- Systemic VU0810464 administration reduces stress-induced hyperthermia but does not impact elevated plus maze performance in mice.

What is the clinical significance

- VU0810464 is a new tool for investigation of neuronal $K_{ir}3$ channel contributions to complex behaviour.

To address the deficits of available neuronal $K_{ir}3$ channel modulators, we investigated a wide variety of non-urea linkers with the goal of improving pharmacokinetic properties and selectivity, while maintaining or improving the potency and efficacy for $K_{ir}3$ channel activation (Wieting et al., 2017). The most productive outcome of these medicinal chemistry studies arose from replacement of the urea linker with phenyl acetamide, leading to the discovery of a novel $K_{ir}3.1$-containing $K_{ir}3$ channel activator, VU0810464 (Wieting et al., 2017). VU0810464 displays nanomolar potency as a $K_{ir}3.1/3.2$ activator as measured by a thallium (Tl^+) flux assay in HEK-293 cells stably expressing $K_{ir}3$ channels and has improved brain distribution relative to ML297 in in vivo pharmacokinetic studies in mice.

Here, we characterized VU0810464 in mouse cultured hippocampal (HPC) neurons and isolated sino-atrial nodal (SAN) cells, native cell types expressing $K_{ir}3.1/3.2$ and $K_{ir}3.1/3.4$ channel subtypes, respectively (Lee et al., 2018; Wydeven, Young, Mirkovic, & Wickman, 2012). We found that VU0810464 is as potent and efficacious as ML297 in activating neuronal $K_{ir}3$ channels but markedly less potent than ML297 in terms of cardiac $K_{ir}3$ channel activation. Furthermore, systemic administration of either ML297 or VU0810464 in mice reduced stress-induced hyperthermia (SIH), a physiological test of anxiolytic efficacy (Adriaan Bouwknecht, Olivier, & Paylor, 2007). Unlike ML297, however, VU0810464 did not decrease anxiety-related behaviour as measured in the elevated plus maze (EPM) test, a standard ethological-based test of anxiety-related behaviour in rodents. The differential impact of VU0810464 in SIH and EPM models supports the contention that these tests afford complementary but distinct assessments of anxiety-related behaviour (Hayashida, Oka, Mera, & Tsuji, 2010; Rodgers, Cole, & Harrison-Phillips, 1994) and suggests that distinct $K_{ir}3$ channel subtypes shape the outcomes of these tests.

2 | METHODS

2.1 | Animal care and use

Animal experiments were approved by the Institutional Animal Care and Use Committee at the University of Minnesota and Vanderbilt University. Animal studies are reported in compliance with the ARRIVE and *BJP* guidelines (Kilkenny, Browne, Cuthill, Emerson, & Altman, 2010). Male and female C57BL/6J mice purchased from the Jackson Laboratory (Bar Harbor, ME, RRID:IMSR_JAX:000664), inbred C57BL/6J mice, and *Kcnj3* (*Girk1*)$^{-/-}$ mice and their wild-type siblings generated on site were used for establishing HPC cultures and isolated SAN cells. The generation of *Kcnj3*$^{-/-}$ mice was as described previously (Bettahi, Marker, Roman, & Wickman, 2002, RRID: MMRRC_031758-UCD). The *Kcnj3* null mutation was backcrossed against the C57BL/6J strain for >20 generations before establishing the crosses used in this study. Male C57BL/6J mice were purchased from Harlan Laboratories (Indianapolis, IN) for in vivo pharmacokinetic studies and from the Jackson Laboratory for the EPM and a cohort of SIH studies. For SIH and EPM studies, purchased mice were allowed to acclimate for 2 weeks before experimental testing to avoid significant transportation influences. *Kcnj3*$^{-/-}$ mice and their wild-type littermates were used for a cohort of SIH studies.

2.2 | Cultured hippocampal neurons

Primary cultures of hippocampal (HPC) neurons were prepared as described previously (Marron Fernandez de Velasco et al., 2017). Briefly, extracted hippocampi from neonatal (P0–3) pups were placed into an ice-cold modified HBSS (Thermo Fisher), 10-mM HEPES-NaOH pH 7.3 (Thermo Fisher), 0.02% (*w*/*v*) Pluronic F-127, and 1.5-μM Thallos-AM (TEFlabs, Austin, TX). The tissue was digested for 20 min with papain and DNAse I at 37°C with occasional inversion. Hippocampi were mechanically dissociated in growth medium containing Neural-basal A medium, 2% B27 supplement, 0.5-mM Glutamax, and antibiotic/antimycotic (Thermo Fisher Scientific) using trituration in 1-ml pipettes. Neurons were pelleted by centrifugation and plated onto 8-mm glass coverslips precoated with poly-L-lysine in 48-well plates. Neurons were maintained in culture in a humidified 5% CO_2 incubator at 37°C, and half of the medium was replaced with fresh growth medium every 3–4 days. Neurons were kept in culture for 10–12 days before experimentation.

2.3 | Sino-atrial node cells

SAN cells were isolated from adult (8–12 weeks) mice as previously described (Anderson et al., 2018). Briefly, mice were anaesthetized with ketamine (100 mg·kg^{-1} i.p.) and xylazine (10 mg·kg^{-1} i.p.), and hearts were excised into Tyrode's solution. SAN-containing tissue was excised into a modified Tyrode's solution containing 140-mM NaCl, 5.4-mM KCl, 1.2-mM KH_2PO_4, 0.2-mM $CaCl_2$, 50-mM taurine, 18.5-mM glucose, 5-mM HEPES, and 0.1% BSA (pH 6.9), with elastase (0.3 mg·ml^{-1}, Worthington Biochemical Corp., Lakewood, NJ) and collagenase II (0.21 mg·ml^{-1}). SAN tissue was digested for 30 min at 37°C and then triturated in wash solution and plated onto laminin-coated coverslips. After plating, SAN cells were used within 8 hr.

2.4 | Electrophysiology

Coverslips containing HPC neurons or SAN cells were transferred to a chamber containing a low-K^+ bath solution consisting of 130-mM NaCl, 5.4-mM KCl, 1-mM $CaCl_2$, 1-mM $MgCl_2$, 5.5-mM D-glucose, and 5-mM HEPES/NaOH (pH 7.4). Pyramidal-shaped neurons with capacitance values between 100 and 200 pF were targeted for hippocampal recordings. SAN cells were identified as thin, striated cells with capacitance values less than 50 pF. Fire-polished borosilicate patch pipettes (4–6 MΩ) were filled with K-gluconate pipette solution containing 140-mM K-gluconate, 2-mM $MgCl_2$, 1.1-mM EGTA, 5-mM HEPES, 2-mM Na_2-ATP, 0.3-mM Na-GTP, and 5-mM phosphocreatine (pH 7.2). Upon achieving whole-cell access, cells were held in voltage-clamp mode at −70 mV. The liquid-junction potential, predicted to be −17 mV using JPCalc software (Molecular Devices, LLC, Sunnyvale, CA), was not corrected. $K_{ir}3$ currents were measured in a high-K^+ bath solution containing 120-mM NaCl, 25-mM KCl, 1-mM $CaCl_2$, 1-mM $MgCl_2$, 5.5-mM D-glucose, and 5-mM HEPES/NaOH (pH 7.4). VU0810464 and ML297 were dissolved in DMSO and then diluted with the high-K^+ bath solution (0.1–0.3% DMSO). **Baclofen** and **carbachol** were dissolved in the high-K^+ bath solution. Compounds were applied directly to the recorded cell using a ValveLink 8.2 rapid perfusion system (AutoMate Scientific, Inc.; Berkeley, CA). For hippocampal recordings, whole-cell currents were measured with hardware (Axopatch-200B amplifier, Digidata 1322A) and software (pCLAMP v. 8.2, RRID:SCR_011323) from Molecular Devices. All currents were low-pass filtered at 2 kHz, digitized at 10 kHz, and stored on computer hard disk for subsequent analysis. Recordings for SAN cells experiments were obtained with hardware (Axopatch-700B amplifier, Digidata 1440A) and software (pCLAMP v. 10.4) from Molecular Devices. Only experiments in which the access resistances were stable (change <20%) and low (<20 MΩ) were included in the analysis.

2.5 | Pharmacokinetics

In vitro pharmacokinetic testing was performed by Q^2 Solutions (Morrisville, NC). For in vivo pharmacokinetic testing, a microsuspension of VU0810464 in 20% (*w*/*v*) β-hydroxypropyl cyclodextrin in sterile water was administered i.p. to male C57BL/6J mice (22.4 ± 1.0 g) at a dose of 30 mg·kg^{-1}. At selected time intervals (15, 30, 45, or 60 min post-injection), mice were killed using CO_2, and brains and plasma were collected. Four mice were used for each group. Analysis of brain and plasma samples was performed by Precera Biosciences (Franklin, TN) as previously described (Wenthur et al., 2013; Wieting et al., 2017).

2.6 | Stress-induced hyperthermia

Young adult (8–12 weeks) male C57BL/6J mice were evaluated in the SIH test, as described previously (Wydeven, Marron Fernandez de Velasco, et al., 2014). Mice were single-housed a day prior to testing, a condition that has been shown to increase basal anxiety (Adriaan Bouwknecht et al., 2007; Groenink, Vinkers, van Oorschot, & Olivier, 2009). Mice were assigned randomly to different treatment groups and were injected i.p. with 10 ml·kg^{-1} of a microsuspension of 0-, 3-, 10-, or 30-mg·kg^{-1} VU0810464 in 20% β-hydroxypropyl cyclodextrin in sterile water, 30 min before testing (Gad, Cassidy, Aubert, Spainhour, & Robbe, 2006). Subsequently, an initial rectal temperature (T_1) was determined using a RET-3 rectal probe (Physitemp Instruments, Clifton, NJ). The probe was dipped into silicon oil, inserted ~1.5 cm into the rectum, and held until a stable rectal temperature was observed (~20 s). Mice were then returned to their home cage for 10 min, followed by a second rectal temperature measurement (T_2). The difference between the second and first temperature measurements was determined ($\Delta T = T_2 - T_1$) and evaluated across treatment groups. Experimenters were blinded to the dose treatment while performing and analysing the data. To determine if the response was $K_{ir}3$ dependent, SIH tests were conducted using a cohort of male and female wild-type and *Kcnj3*$^{-/-}$ siblings (8–12 weeks) generated in our colony. A low initial temperature (T_1 < 35°C) of the animals may affect the ΔT and thus these animals were excluded for further analysis.

2.7 | Elevated plus maze and open-field testing

Mice were acclimatized to and handled within the test room for 2 days prior to testing. On the test day, mice received 10 ml·kg^{-1} of a microsuspension of VU0810464 (3–30 mg·kg^{-1}), evaluated using two different vehicles (20% β-hydroxypropyl cyclodextrin in sterile water and 0.5% hydroxypropyl cellulose/4% DMSO in saline). Thirty minutes after this i.p. injection, mice were placed in the EPM centre (facing the open arm and away from the experimenter), and their activity was recorded for 5 min by a video camera. Tracking and data analysis were performed using ANY-maze (v. 5.2) software (Stoelting Co., Wood Dale, IL). Time spent in the open arms, closed arms, and centre, as well as the entries to the open and closed arms and total distance travelled, was assessed. After the EPM test, mice were placed in automated open-field activity chambers and allowed to explore for 15 min. Thigmotaxis, open zone entries, total distance travelled, and stereotypy counts for each mouse were recorded and analysed using the Activity Monitor software (Med-Associates, Inc; St. Albans, VT). Experimenters were blinded to the dose treatment while performing and analysing the data. For the EPM data, animals that fell out of the maze or travelled a low total distance (less than 5 m) were excluded from the data subjected to analysis.

2.8 | Data and statistical analysis

The data and statistical analysis comply with the recommendations on experimental design and analysis in pharmacology (Curtis et al., 2018). Statistical analyses for group comparisons were only undertaken if group sizes were five or larger. Furthermore, the group size was designed to be equal and was based on the expected difference in a desired endpoint measurement from our pilot studies and from the mean and SEM reported in our previous publication (Wydeven, Marron Fernandez de Velasco, et al., 2014). Data are presented throughout as the mean ± SEM. Statistical analyses were performed using Prism 5 (GraphPad Software, Inc.; La Jolla, CA, RRID: SCR_002798). Data were analysed with Student's two-tailed *t* test, one-way ANOVA, or two-way ANOVA, as appropriate. Tukey and Bonferroni multiple comparison post hoc tests were used only if *F* was significant and there was no variance inhomogeneity. Differences were considered significant if $P < 0.05$. Data points that fell outside of the group mean ± 2 *SDs* were excluded from final analysis.

2.9 | Chemicals

Unless otherwise noted, chemicals were purchased from Millipore-Sigma (St. Louis, MO).

2.10 | Nomenclature of targets and ligands

Key protein targets and ligands in this article are hyperlinked to corresponding entries in http://www.guidetopharmacology.org, the common portal for data from the IUPHAR/BPS Guide to PHARMACOLOGY (Harding et al., 2018), and are permanently archived in the Concise Guide to PHARMACOLOGY 2017/18 (Alexander, Christopoulos et al., 2017; Alexander, Peters et al., 2017).

3 | RESULTS

3.1 | Characterization of VU0810464 in heterologously expressed and native $K_{ir}3$ channels

Synthesis and testing of over 200 newly analogues led to the discovery of VU0810464 (Wieting et al., 2017), which carries a novel chemical scaffold distinct from ML297-like urea compounds (Figure S1A,B). VU0810464 was >3-fold more potent on $K_{ir}3.1/3.2$-expressing HEK-293 cells compared to $K_{ir}3.1/3.4$-expressing cells, as measured using a Tl^+ flux assay (Figure S1C,D). Additionally, preliminary tests suggested that the compound might have improved potency and selectivity compared to ML297 and thus warranted further exploration in native cell types expressing $K_{ir}3$ channels (Figure S1D).

We utilized whole-cell patch-clamp electrophysiology to measure the efficacy and potency of VU0810464 in activating $K_{ir}3$ channels in cultured HPC neurons, which primarily express $K_{ir}3.1/3.2$ channels (Wydeven, Marron Fernandez de Velasco, et al., 2014; Wydeven et al., 2012). VU0810464 evoked a concentration-dependent inward current in HPC neurons from wild-type mice, and this current was reversed by application of 0.3-mM Ba^{2+}, which blocks inwardly rectifying K^+ channels (Figure 1a). To confirm that the response is $K_{ir}3$-dependent, we measured whole-cell currents evoked by a saturating

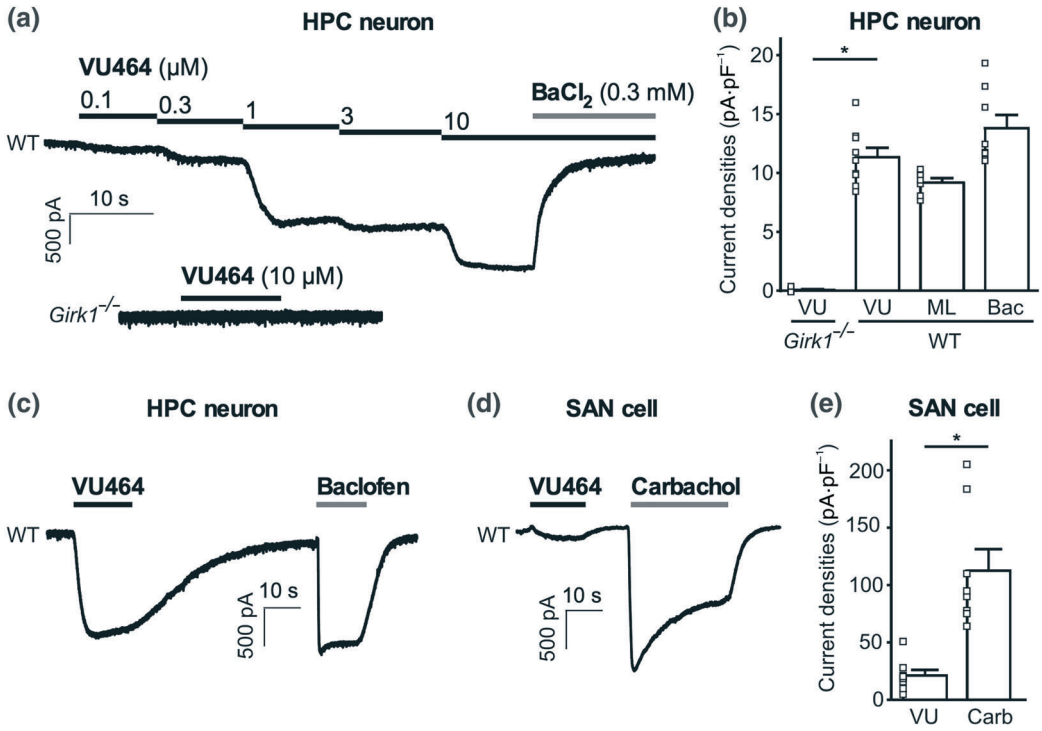

FIGURE 1 Electrophysiological characterization of VU0810464 (VU464) in cultured HPC neurons and isolated SAN cells. (a) Top, representative trace for the concentration-dependent response experiment of VU0810464-evoked current in a wild-type (WT) cultured HPC neuron, and this current was reversed by bath application of 0.3-mM Ba^{2+}, an inwardly rectifying K^+ channel blocker. Bottom, representative trace of VU0810464 at a saturating concentration (10 μM) in a *Kcnj3*$^{-/-}$ HPC neuron. (b) Summary of peak current densities evoked by 10-μM VU0810464 in WT (n = 9) and *Kcnj3*$^{-/-}$ (n = 6) HPC neurons and by saturating concentrations of ML297 (ML, 10 μM, n = 7) and the $GABA_B$ receptor agonist baclofen (Bac, 100 μM, n = 8). Individual data points are represented as small squares overlapping the relevant bar in the plot. One-way ANOVA with Tukey's multiple comparison test. *P < .05. (c, d) Representative traces showing whole-cell currents evoked by a maximal concentration of VU0810464 (10 μM for neurons and 30 μM for SAN cells), following by the application of a GPCR agonist at saturating concentration in cultured HPC neurons and SAN cells. Baclofen (100 μM) and the non-selective muscarinic receptor agonist carbachol (10 μM) were used in neurons and SAN cells, respectively. (e) Summary of peak current densities evoked by 30-μM VU0810464 (VU, n = 8) and 10-μM carbachol (Carb, n = 8) in SAN cells from WT mice. Unpaired two-tailed t test. *P < 0.05

concentration of VU0810464 (10 μM) in HPC neurons from *Kcnj3*$^{-/-}$ mice; we did not observe responses in K_{ir}31-lacking neurons (Figure 1a,b). Maximal VU0810464-induced currents in wild-type cultures were similar in magnitude to maximal ML297-evoked currents (Figure 1b).

Next, we sought to compare the efficacies of VU0810464 in activating K_{ir}3 channels in neurons relative to cardiac myocytes. Since HPC neurons and cardiac SAN cells are two distinct cell systems, we used within-cell internal controls to measure the magnitude of currents evoked by VU0810464 relative to that evoked by standard agonists in neurons and cardiac myocytes. Specifically, VU0810464-induced currents were compared with currents evoked by either the $GABA_B$ receptor agonist baclofen (HPC neurons) or the muscarinic (M_2) receptor agonist carbachol (SAN cells), standard agonists that evoke robust and reliable K_{ir}3 currents in neurons and cardiac myocytes, respectively (Wydeven, Posokhova, et al., 2014; Wydeven et al., 2012). In HPC neurons, currents evoked by 10-μM VU0810464 were similar to those evoked by a saturating concentration of baclofen (Figure 1b,c; Marron Fernandez de Velasco et al., 2017). In contrast, currents evoked by a saturating concentration of VU0810464 (30 μM) in SAN cells were significantly smaller than maximal carbachol-induced currents (Figure 1d,e; Wydeven, Posokhova, et al., 2014).

We also assessed the selectivity of VU0810464 for neuronal versus cardiac K_{ir}3 channels by comparing potencies of VU0810464-induced responses in HPC neurons and SAN cells. VU0810464 demonstrated a ~9-fold higher potency for K_{ir}3 channel activation in neurons as compared to SAN cells (Figure 2a,b). VU0810464 was as potent as ML297 in terms of activating the K_{ir}3 channel in HPC neurons but was significantly less potent than ML297 in activating the K_{ir}3 channel in SAN cells, indicating a significant improvement in neuronal K_{ir}3 channel subtype selectivity for VU0810464 as compared to ML297 (Figure 2b). Based on these promising electrophysiological profiles, we proceeded to evaluate the compound in in vivo pharmacokinetic studies.

3.2 | *In vivo* pharmacokinetic characterization of VU0810464

Since VU0810464 and ML297 are lipophilic compounds that have low aqueous solubilities at concentrations desired for intraperitoneal

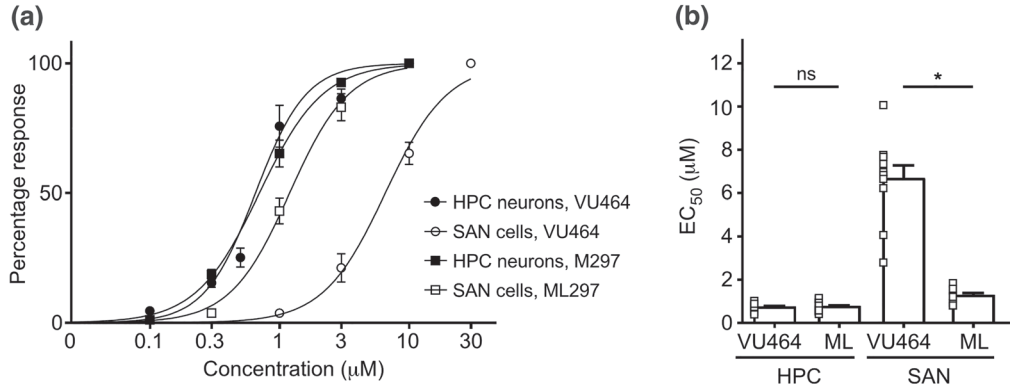

FIGURE 2 Selectivity of VU0810464 (VU464) for neuronal over cardiac $K_{ir}3$ channels. (a) Concentration-dependent response curves of currents evoked by VU0810464 (n = 8) and ML297 (n = 12) in HPC neurons as well as SAN cells (VU464: n = 10; M297: n = 8). (b) Summary of EC_{50} values of VU0810464- and ML297-induced currents in HPC neurons and SAN cells. Individual data points are represented as small squares overlapping the relevant bar in the plot. One-way ANOVA with Tukey's multiple comparison test. *P < 0.05; ns, not significant

dosing, we sought to identify a vehicle that could improve their solubilities. We tested a number of compounds often used as components of vehicle for in vivo studies including Tween, polyethylene glycol, Labrasol, and β-hydroxypropyl cyclodextrin. Among these options, the only formulation resulting in a VU0810464 solution (at 10 mg·kg^{-1}—the dose at which we observed the anxiolytic efficacy with ML297) was a Labrasol-based vehicle. Unfortunately, this formulation was poorly tolerated by mice, with a number of the animals dying when vehicle alone was injected. Accordingly, we used a microsuspension approach to deliver compounds to mice. For the initial characterization of VU0810464 in pharmacokinetic studies, we used a vehicle containing ethanol (16–18%), PEG400 (64–72%), and DMSO (10–20%; Wieting et al., 2017). In the present study, we switched to use a β-hydroxypropyl cyclodextrin vehicle for most of the in vivo experiments to avoid the potential influence of DMSO on experimental endpoints (Colucci et al., 2008; Galvao et al., 2014). β-Hydroxypropyl cyclodextrin is also an approved excipient of drug formulations, and it was sufficient to yield a relatively stable microsuspension of both VU0810464 and ML297 over the timeframe of our in vivo studies (Abney et al., 2019; Gould & Scott, 2005).

Intraperitoneal dosing of a microsuspension of VU0810464 (30 mg·kg^{-1}) revealed that it displayed a favourable distribution to the brain (unbound brain to plasma ratio, $K_{p,uu}$ = 0.83; Figure 3b). This finding represents a remarkable improvement over ML297, which exhibits a low brain distribution ($K_{p,uu}$ = 0.32). Clearance of VU0810464 was rapid, however, with brain and plasma half-lives of ~20 min (Figure 3a,b). In contrast, the brain and plasma half-lives of ML297 were ~40 min. Despite the decrease in half-life of

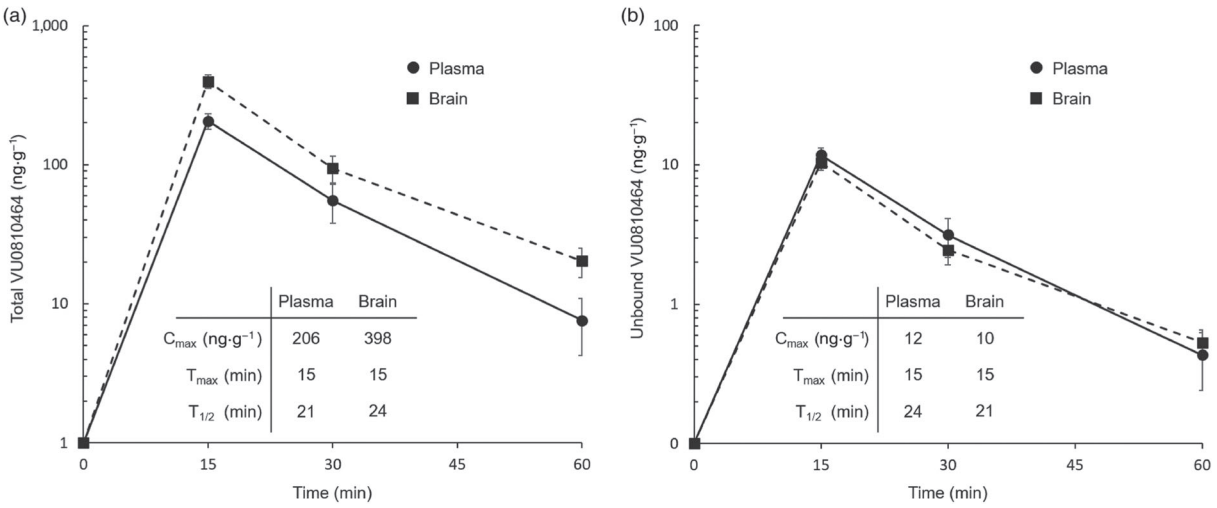

FIGURE 3 Plasma and brain time course of VU0810464. Shown are plasma and brain levels of VU0810464 after i.p. dosing. Mice received i.p. injections of a microsuspension of 30-mg·kg^{-1} VU0810464 in 20% (*w*/*v*) β-hydroxypropyl cyclodextrin in water. (a) Total plasma levels and total brain levels. (b) Unbound plasma levels corrected for plasma protein binding and unbound brain levels corrected for brain homogenate binding. Data are the average for four separate animals. Error ranges represent the *SEM*

VU0810464 compared to ML297, the enhanced selectivity of VU0810464 for neuronal over cardiac $K_{ir}3$ channels, as well as the improved brain distribution, prompted evaluation of in vivo efficacy.

3.3 | Effect of VU0810464 in anxiety-related behavioural tests

Previously, we reported that ML297 (30 mg·kg^{-1} i.p.) evoked a dose-dependent, Kir3-dependent decrease in anxiety-related behaviour, as assessed using the SIH and EPM tests (Wydeven, Marron Fernandez de Velasco, et al., 2014). Thus, we compared the efficacy of VU0810464 and ML297 in these tests, using C57BL/6J mice.

In the SIH paradigm, stressors (i.e., restraint and rectal temperature measurement) cause an increase in total body temperature, a motor-activity-independent physiological response caused by stress. Anxiolytic drugs, such as diazepam, blunt this stress-induced response (Vinkers et al., 2008; Zethof, Van der Heyden, Tolboom, & Olivier, 1995). We started by validating our SIH assay with diazepam. We observed that diazepam (4 mg·kg^{-1} i.p.) produced a robust suppression of SIH in male C57BL/6J mice (Figure S2A), without impacting the initial/pre-stressor temperature measurement (T_1 value; Figure S2B). Similarly, VU0810464 and ML297 produced a dose-dependent reduction of SIH response (Figure 4a,b), without impacting baseline temperature. To test if VU0810464, like ML297 (Wydeven, Marron Fernandez de Velasco, et al., 2014), mediates its effect through Kir3 channel activation, SIH tests were conducted using a cohort of male and female wild-type and congenic *Kcnj3*$^{-/-}$ siblings. While VU0810464 (10 mg·kg^{-1} i.p.) suppressed the SIH response in wild-type mice, it had no impact on *Kcnj3*$^{-/-}$ mice (Figure 4c).

We next compared the impact of VU0810464 in the EPM, a standard ethologically based test of anxiety in rodents based on their natural aversion to open spaces and heights (Calhoon & Tye, 2015; Lister, 1990). Diazepam reduced anxiety-related behaviour in C57BL/6J mice, as measured by increased time spent in the open arms, and decreased time spent in the close arms, of the EPM (Figure S3). In contrast, VU0810464 (3–30 mg·kg^{-1} i.p.) had no impact on EPM performance (Figure 5a). Similarly, VU0810464 (30 mg·kg^{-1} i.p.) did not impact thigmotaxis or total distance travelled in an open-field test (Figure 5b). Given these unexpected negative outcomes, we also evaluated ML297 in the EPM, at a dose (30 mg·kg^{-1} i.p.) shown previously to decrease anxiety-related behaviour (Wydeven, Marron Fernandez de Velasco, et al., 2014); ML297 was similarly ineffective in this test (Figure 5c).

To discern whether the choice of vehicle impacted efficacy in the EPM test, we re-evaluated both VU0810464 and ML297 in the vehicle (0.5% hydroxypropyl cellulose/4% DMSO in saline) used previously to evaluate the impact of ML297 on motor activity and mood-related tests (Wydeven, Marron Fernandez de Velasco, et al., 2014). While the VU0810464 microsuspension in the hydroxypropyl cellulose/DMSO vehicle was still without effect in the EPM test, ML297 (30 mg·kg^{-1} i.p.) did increase time spent in the open arms of the EPM, consistent with our previous findings (Figure 5d,e). Thus, ML297 (but not VU0810464) exhibits vehicle-dependent anxiolytic efficacy in the EPM test.

4 | DISCUSSION

Efforts from medicinal chemistry studies and high-throughput screens led to the development of VU0810464, a non-urea-based $K_{ir}3$ channel activator with improved brain penetration as compared to the previously reported urea-containing $K_{ir}3$ channel activators, including ML297 (Wieting et al., 2017). While the high-throughput nature of Tl^+ flux-based analysis in HEK-293 cells is useful for screening libraries of compounds, these assays have relatively low temporal resolution and information content (Gill et al., 2017; Yu, Li, Wang, & Wang, 2016; Zou et al., 2010). In addition, HEK-293 cells may lack factors that impact the efficiency of the compound for channel activation. These limitations highlight the importance of evaluating compound performance in native cell types that normally express $K_{ir}3$ channels. While the electrophysiological studies herein revealed no improvement in potency of VU0810464 as compared to ML297 in HPC neurons, the selectivity profile obtained in HPC neurons and SAN cells was consistent with the Tl^+ flux data, demonstrating a significantly higher potency of VU0810464 in neurons compared to cardiac myocytes.

While a previous study investigated the impact of ML297 on hippocampal cultures (Wydeven, Marron Fernandez de Velasco, et al., 2014), it was not clear how this compound effects cardiac myocytes, where $K_{ir}3$ channels contribute to heart rate regulation. Here, we showed that VU0810464 exhibits relative low potency for ($K_{ir}3.1$/3.4) $K_{ir}3$ channels in SAN cells, relative to ML297 (Figure 2a,b). VU0810464, therefore, represents a potentially useful tool for selective targeting of neuronal ($K_{ir}3.1$/3.2) $K_{ir}3$ channels.

Systemic administration of VU0810464, like ML297, reduces the SIH response in mice. The SIH response represents a conserved autonomic change associated with high-anxiety state (Vinkers et al., 2008). Anxiolytic drugs such as benzodiazepines, **5-HT$_{1A}$ receptor** agonists, and alcohol have been shown to reduce SIH. Since $K_{ir}3$ channels are downstream effectors of 5-HT_{1A} receptors (Luscher, Jan, Stoffel, Malenka, & Nicoll, 1997; Raymond, Mukhin, Gettys, & Garnovskaya, 1999), the anxiolytic effect of 5-HT_{1A} receptor agonists might be mediated through $K_{ir}3$ channel activation. Indeed, in dorsal raphe neurons from *Kcnj6* (*Girk2*)$^{-/-}$ mice, the inhibitory effect of the 5-HT_{1A} receptor agonist, 8-OH-DPAT, was blunted (Llamosas, Bruzos-Cidon, Rodriguez, Ugedo, & Torrecilla, 2015). In addition, citalopram (a selective 5-HT reuptake inhibitor) showed reduced antidepressant effect in *Kcnj6 (Girk2)*$^{-/-}$ mice (Llamosas et al., 2015). Further investigation of the contribution of $K_{ir}3$ channels to $5HT_{1A}$ receptor-dependent signalling could reveal important cellular and/or molecular targets that could be exploited to treat neurological problems linked to dysfunctional 5-HT transmission.

Consistent with our previous report (Wydeven, Marron Fernandez de Velasco, et al., 2014), we observed a smaller stress-induced increase in body temperature in vehicle-treated *Kcnj3*$^{-/-}$ mice as compared to vehicle-treated wild-type mice (Figure 4b). This

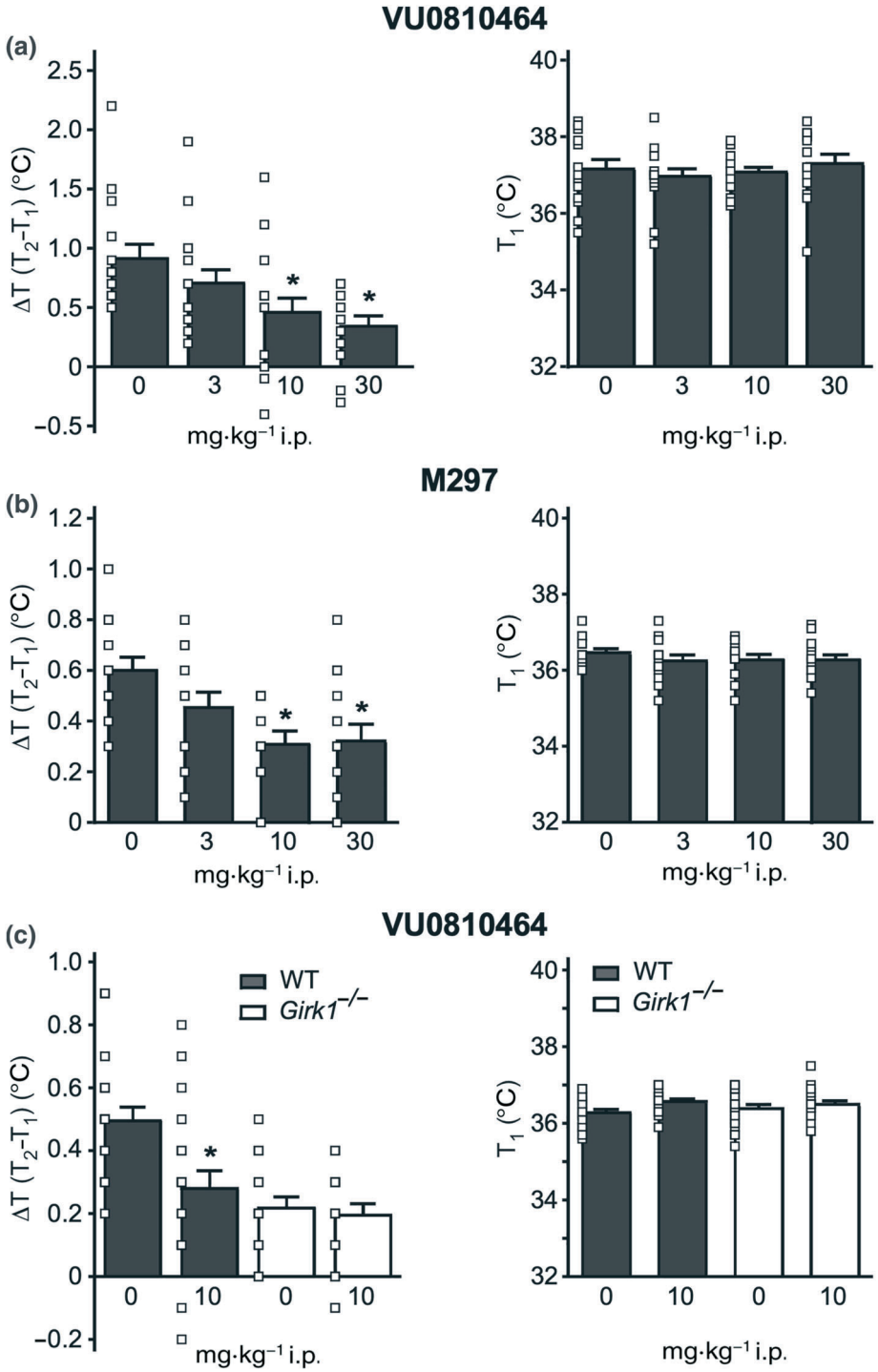

FIGURE 4 Effect of VU0810464 in the SIH test. (a) Left, dose-dependent reduction of stress-induced increase in body temperature from wild-type (WT) male mice receiving i.p. injections of different doses of VU0810464 (0, 3, 10, and 30 mg·kg^{-1} in 20% β-hydroxypropyl cyclodextrin). Individual data points are represented as small squares overlapping the relevant bar in the plot. One-way ANOVA with Tukey's multiple comparison test. *P < 0.05 versus 0 mg·kg^{-1}. n = 15, 16, 17, and 14 for 0, 3, 10, and 30 mg·kg^{-1}, respectively. Right, summary of initial temperature measurements (T_1 values) in those mice. (b) Left, effect of various doses of ML297 (0, 3, 10, and 30 mg·kg^{-1} in 20% β-hydroxypropyl cyclodextrin, i.p.) in SIH test in WT male mice. One-way ANOVA with Tukey's multiple comparison test. *P < 0.05 versus 0 mg·kg^{-1}. n = 14, 13, 12, and 14 for 0, 3, 10, and 30 mg·kg^{-1}, respectively. Right, summary of initial temperature measurements (T_1 values) in those WT mice. (c) Left, effect of VU0810464 (0 or 10 mg·kg^{-1} i.p., in 20% β-hydroxypropyl cyclodextrin) on SIH in WT and *Kcnj3*$^{-/-}$ mice containing balanced numbers of female and male mice. There was no sex effect, so male and female data were pooled. Two-way ANOVA with Bonferroni post-tests. *P < 0.05 versus 0 mg·kg^{-1} in WT. n = 19, 17, 20, and 19 for 0 mg·kg^{-1} in WT, 10 mg·kg^{-1} in WT, 0 mg·kg^{-1} in *Kcnj3*$^{-/-}$, and 10 mg·kg^{-1} in *Kcnj3*$^{-/-}$ mice, respectively. Right, summary of initial temperature measurements in those WT and *Kcnj3*$^{-/-}$ mice

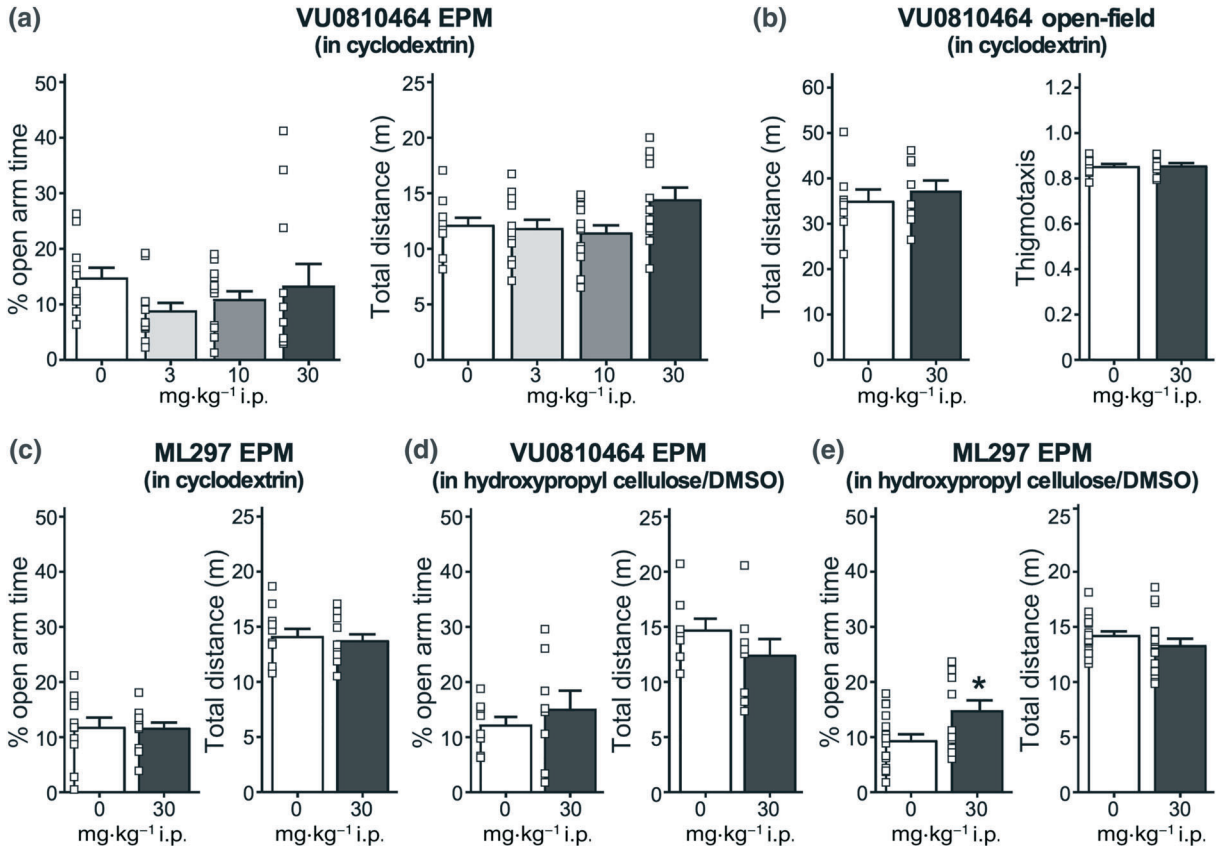

FIGURE 5 VU0810464 had no effect in the EPM and open-field tests. (a) Summaries of percentage of time spent in open arms (left) and total distance travelled (right) from mice receiving injections of different doses of VU0810464 (0, 3, 10, and 30 mg·kg^{-1} i.p., in 20% β-hydroxypropyl cyclodextrin). Individual data points are represented as small squares overlapping the relevant bar in the plot. One-way ANOVA with Tukey's multiple comparison test. n = 11, 12, 13, and 11 for 0, 3, 10, and 30 mg·kg^{-1}, respectively. (b) Summaries of thigmotaxis (right, ratio of distance travelled in the periphery to total distance travelled in a brightly lit open-field arena) and total distance travelled (left) from mice receiving i.p. injections of 30-mg·kg^{-1} VU0810464 (in 20% β-hydroxypropyl cyclodextrin, n = 8) or vehicle alone (n = 8). Student's two-tailed t test. (c) Summaries of percentage of time spent in open arms (left) and total distance travelled (right) from mice receiving i.p. injections of 30-mg·kg^{-1} ML297 (in 20% β-hydroxypropyl cyclodextrin, n = 11) or vehicle alone (n = 11). Student's two-tailed t test. (d) Summaries of percentage of time spent in open arms (left) and total distance travelled (right) from mice receiving i.p. injections of 30-mg·kg^{-1} VU0810464 (in 0.5% hydroxypropyl cellulose/4% DMSO, n = 8) or vehicle alone (n = 8). Student's two-tailed t test. (e) Summaries of percentage of time spent in open arms (left) and total distance travelled (right) from mice receiving i.p. injections of 30-mg·kg^{-1} ML297 (in 0.5% hydroxypropyl cellulose/4% DMSO, n = 16) or vehicle alone (n = 13). Student's two-tailed t test. *P < 0.05 versus 0 mg·kg^{-1}

suggests that $K_{ir}3$ channels may play a role in regulating body temperature under stressful conditions. The blunted SIH response in vehicle-treated *Kcnj3*$^{-/-}$ mice limits our ability to interpret the experiments with VU0810464, since the lack of effect following VU0810464 administration in *Kcnj3*$^{-/-}$ mice may be attributable to a floor effect. However, previous studies suggest that $K_{ir}3$ channels mediate the hypothermic effect of several inhibitory GPCR agonists (Costa, Stasko, Stoffel, & Scott-McKean, 2005; Jacobson & Cryan, 2005). This evidence, together with our findings showing the same SIH effect with opposing $K_{ir}3$ channel manipulations (i.e., genetic ablation vs. pharmacological activation), suggests that an optimal range of $K_{ir}3$-dependent signalling is required for the autonomic change associated with a high-anxiety state.

We observed different magnitudes of SIH response in purchased C57BL/6J mice and *Kcnj3*$^{+/+}$ (control) mice generated in our colony from crosses of *Kcnj3*$^{+/-}$ mice (Figure 4a,b); *Kcnj3*$^{+/+}$ mice responded less in the SIH test compared to purchased C57BL/6J mice. This difference might be caused by different breeding environments and the transferring process from Jackson Laboratory to our institution. Notably, these studies were performed by two different experimenters in two different laboratory settings, which might explain the different magnitude of the SIH response. Despite the difference in magnitude of the SIH response, both studies show a significant reduction in SIH in mice administered VU0810464 as compared to control/vehicle.

An intriguing aspect of this study is the finding that the efficacy of ML297 in the EPM test was sensitive to vehicle. As discussed above, we opted to use β-hydroxypropyl cyclodextrin in our current study since it is an approved excipient of drug formulations in the United States and Europe, and it is recommended for use as solubilizer and stabilizer for oral formulations (Gould & Scott, 2005). β-Hydroxypropyl cyclodextrin did appear to be better in generating a fine VU0810464 microsuspension than hydroxypropyl cellulose/DMSO, the vehicle

used in our previous study of ML297. Compound preparation in the β-hydroxypropyl cyclodextrin vehicle did require prolonged sonication (~45 min) at 37°C, however, which was not required with the hydroxypropyl cellulose/DMSO vehicle. Thus, subtle differences in the nature of the microsuspensions, and/or stabilities of the compound in different vehicles, might underlie the vehicle-dependent efficacy of ML297 in EPM test.

Surprisingly, VU0810464, unlike ML297, did not impact EPM performance in mice (Figure 5). This may be due to a faster elimination rate of VU0810464 as compared to ML297. Indeed, as the rapid clearance of VU0810464 will likely limit its broad utility in vivo, ongoing studies are utilizing the VU0810464 scaffold to develop selective and stable $K_{ir}3.1/3.2$ channel activators. Another potential explanation for the differential behavioural outcomes of ML297 and VU0810464 in the EPM test relates to the $K_{ir}3$ channel subtype(s) impacting EPM-related behaviour. While the $K_{ir}3.1/3.2$ subtype is often considered to be the prototypical neuronal $K_{ir}3$ channel, other neuronal $K_{ir}3$ channel subtypes have been described (Lujan & Aguado, 2015), including $K_{ir}3.4$-containing channels (Wickman, Karschin, Karschin, Picciotto, & Clapham, 2000); these $K_{ir}3$ channel subtypes may be more relevant than $K_{ir}3.1/3.2$ channels to EPM-related behaviour. Moreover, the potential impact of the $K_{ir}3.3$ subunit on the sensitivity of neuronal $K_{ir}3$ channels to ML297, VU0810464, and related compounds is unclear. Thus, the lack of apparent anxiolytic efficacy of VU0810464 in the EPM test may reflect its improved selectivity for $K_{ir}3.1/3.2$ channels.

The differential impact of VU0810464 on performance in EPM and SIH tests suggests a dissociation between the two models. Interestingly, the original SIH paradigm involved group-housed mice, with those removed last from the home cage displaying elevated body temperature compared to those removed first (Borsini, Lecci, Volterra, & Meli, 1989). This "cohort removal" phenomenon has been proposed as a model of anticipatory anxiety and is prevented by anxiolytics and enhanced by anxiogenics (Lecci, Borsini, Mancinelli, et al., 1990; Lecci, Borsini, Volterra, & Meli, 1990). Cohort removal, however, does not impact EPM performance in mice (Rodgers et al., 1994). In addition, a more recent study showed that repeated social defeat stress induced chronic hyperthermia and increased depression-related behaviour in the forced swim test but did not impact EPM performance (Hayashida et al., 2010). Our findings support the contention that SIH and EPM tests afford complementary yet distinct measurements of stress- and anxiety-related behaviour, respectively.

In summary, VU0810464 is a new tool that can be used to investigate the relevance of neuronal $K_{ir}3.1/3.2$ channels to complex behaviours. Furthermore, compounds based on VU0810464 chemical scaffold could prove useful as $K_{ir}3$ channel subtype-selective modulators for treatment of neurological disorders.

ACKNOWLEDGEMENTS

The authors thank Nicholas Carlblom, Zhilian Xia, and Hannah Oberle for exceptional care of the mouse colony at the University of Minnesota. The authors thank the staff of the Vanderbilt High-throughput Screening Facility and Tiffany Farmer and Allison Puglisi in the Vanderbilt Metabolic Physiology Shared Resource for assistance with dosing in the pharmacokinetic studies. This work was supported by National Institutes of Health grants to C.D.W, K.W., and C.R.H. (MH107399), K.W. (HL105550 and DA034696), and A.A. (HL139090). Thallium flux experiments were performed using a Panoptic kinetic imaging plate reader funded by Biomedical Research Support Shared Instrumentation Grant (S10).

CONFLICT OF INTEREST

C.D.W. is an owner of WaveFront Biosciences, manufacturer of the Panoptic, and receives royalties from the sale of Thallos through a licence from Vanderbilt.

AUTHOR CONTRIBUTIONS

K.W., C.D.W., C.R.H., B.V., and E.M.F.d.V. conceived the idea for the project, designed the experiments, and coordinated the work. B.V. performed the electrophysiological studies in neurons, did behavioural studies, analysed data, and prepared the figures. K.K.A. performed thallium flux assays and pharmacokinetic studies. J.S.D. and R.D.M analysed pharmacokinetic data. A.A. performed the electrophysiological studies in cardiac cells. M.B. performed the dose–response experiments of VU0810464 in the stress-induced hyperthermia and the elevated plus maze tests. B.V. wrote the manuscript, with suggestions and revisions from K.W., C.D.W., E.M.F.d.V., and A.A. All authors approved the final version of the manuscript.

DECLARATION OF TRANSPARENCY AND SCIENTIFIC RIGOUR

This Declaration acknowledges that this paper adheres to the principles for transparent reporting and scientific rigour of preclinical research as stated in the *BJP* guidelines for Design & Analysis, and Animal Experimentation, and as recommended by funding agencies, publishers, and other organizations engaged with supporting research.

ORCID

Kevin Wickman https://orcid.org/0000-0002-5179-9540

REFERENCES

Abney, K. K., Bubser, M., Du, Y., Kozek, K. A., Bridges, T. M., Lindsley, C. W., … Weaver, C. D. (2019). Analgesic effects of the GIRK Activator, VU0466551, alone and in combination with morphine in acute and persistent pain models. *ACS Chemical Neuroscience* 2019 March 26. https://doi.org/10.1021/acschemneuro.8b00370. [Epub ahead of print]

Adriaan Bouwknecht, J., Olivier, B., & Paylor, R. E. (2007). The stress-induced hyperthermia paradigm as a physiological animal model for anxiety: A review of pharmacological and genetic studies in the mouse. *Neuroscience and Biobehavioral Reviews*, *31*(1), 41–59. https://doi.org/10.1016/j.neubiorev.2006.02.002

Alexander, S. P. H., Christopoulos, A., Davenport, A. P., Kelly, E., Marrion, N. V., Peters, J. A., … CGTP Collaborators (2017). THE CONCISE GUIDE TO PHARMACOLOGY 2017/18: G protein-coupled receptors. *British Journal of Pharmacology*, *174*(S1), S17–S129. https://doi.org/10.1111/bph.13878

Alexander, S. P. H., Peters, J. A., Kelly, E., Marrion, N. V., Faccenda, E., Harding, S. D., … CGTP Collaborators (2017). THE CONCISE GUIDE TO PHARMACOLOGY 2017/18: Ligand-gated ion channels. *British Journal of Pharmacology*, *174*(S1), S130–S159. https://doi.org/10.1111/bph.13879

Anderson, A., Kulkarni, K., Marron Fernandez de Velasco, E., Carlblom, N., Xia, Z., Nakano, A., … Wickman, K. (2018). Expression and relevance of the G protein-gated K^+ channel in the mouse ventricle. *Scientific Reports*, *8*(1), 1192. https://doi.org/10.1038/s41598-018-19719-x

Berg, R. W., Alaburda, A., & Hounsgaard, J. (2007). Balanced inhibition and excitation drive spike activity in spinal half-centers. *Science*, *315*(5810), 390–393. https://doi.org/10.1126/science.1134960

Bettahi, I., Marker, C. L., Roman, M. I., & Wickman, K. (2002). Contribution of the Kir3.1 subunit to the muscarinic-gated atrial potassium channel IKACh. *The Journal of Biological Chemistry*, *277*(50), 48282–48288. https://doi.org/10.1074/jbc.M209599200

Borsini, F., Lecci, A., Volterra, G., & Meli, A. (1989). A model to measure anticipatory anxiety in mice? *Psychopharmacology*, *98*(2), 207–211. https://doi.org/10.1007/BF00444693

Brewer, C. L., & Baccei, M. L. (2018). Enhanced postsynaptic GABAB receptor signaling in adult spinal projection neurons after neonatal injury. *Neuroscience*, *384*, 329–339. https://doi.org/10.1016/j.neuroscience.2018.05.046

Calhoon, G. G., & Tye, K. M. (2015). Resolving the neural circuits of anxiety. *Nature Neuroscience*, *18*(10), 1394–1404. https://doi.org/10.1038/nn.4101

Colucci, M., Maione, F., Bonito, M. C., Piscopo, A., Di Giannuario, A., & Pieretti, S. (2008). New insights of dimethyl sulphoxide effects (DMSO) on experimental in vivo models of nociception and inflammation. *Pharmacological Research*, *57*(6), 419–425. https://doi.org/10.1016/j.phrs.2008.04.004

Costa, A. C., Stasko, M. R., Stoffel, M., & Scott-McKean, J. J. (2005). G-protein-gated potassium (GIRK) channels containing the GIRK2 subunit are control hubs for pharmacologically induced hypothermic responses. *The Journal of Neuroscience*, *25*(34), 7801–7804. https://doi.org/10.1523/JNEUROSCI.1699-05.2005

Crabtree, G. W., Sun, Z., Kvajo, M., Broek, J. A., Fenelon, K., McKellar, H., … Gogos, J. A. (2017). Alteration of neuronal excitability and short-term synaptic plasticity in the prefrontal cortex of a mouse model of mental illness. *The Journal of Neuroscience*, *37*(15), 4158–4180. https://doi.org/10.1523/JNEUROSCI.4345-15.2017

Curtis, M. J., Alexander, S., Cirino, G., Docherty, J. R., George, C. H., Giembycz, M. A., … Ahluwalia, A. (2018). Experimental design and analysis and their reporting II: updated and simplified guidance for authors and peer reviewers. *British Journal of Pharmacology*, *175*(7), 987–993. https://doi.org/10.1111/bph.14153

Gad, S. C., Cassidy, C. D., Aubert, N., Spainhour, B., & Robbe, H. (2006). Nonclinical vehicle use in studies by multiple routes in multiple species. *International Journal of Toxicology*, *25*(6), 499–521. https://doi.org/10.1080/10915810600961531

Galvao, J., Davis, B., Tilley, M., Normando, E., Duchen, M. R., & Cordeiro, M. F. (2014). Unexpected low-dose toxicity of the universal solvent DMSO. *The FASEB Journal*, *28*(3), 1317–1330. https://doi.org/10.1096/fj.13-235440

Gill, S., Gill, R., Wen, Y., Enderle, T., Roth, D., & Liang, D. (2017). A high-throughput screening assay for NKCC1 cotransporter using nonradioactive rubidium flux technology. *Assay and Drug Development Technologies*, *15*(4), 167–177. https://doi.org/10.1089/adt.2017.787

Gould, S., & Scott, R. C. (2005). 2-Hydroxypropyl-β-cyclodextrin (HP-β-CD): A toxicology review. *Food and Chemical Toxicology*, *43*(10), 1451–1459. https://doi.org/10.1016/j.fct.2005.03.007

Groenink, L., Vinkers, C., van Oorschot, R., & Olivier, B. (2009). Models of anxiety: Stress-induced hyperthermia (SIH) in singly housed mice. *Current Protocols in Pharmacology*. Chapter 5: Unit 5.16

Hayashida, S., Oka, T., Mera, T., & Tsuji, S. (2010). Repeated social defeat stress induces chronic hyperthermia in rats. *Physiology & Behavior*, *101*(1), 124–131. https://doi.org/10.1016/j.physbeh.2010.04.027

Harding, S. D., Sharman, J. L., Faccenda, E., Southan, C., Pawson, A. J., Ireland, S., … NC-IUPHAR (2018). The IUPHAR/BPS Guide to PHARMACOLOGY in 2018: updates and expansion to encompass the new guide to IMMUNOPHARMACOLOGY. *Nucleic Acids Research*, *46*(D1), D1091–D1106.

Huang, Y., Zhang, Y., Kong, S., Zang, K., Jiang, S., Wan, L., … Wang, Y. (2018). GIRK1-mediated inwardly rectifying potassium current suppresses the epileptiform burst activities and the potential antiepileptic effect of ML297. *Biomedicine & Pharmacotherapy*, *101*, 362–370. https://doi.org/10.1016/j.biopha.2018.02.114

Jacobson, L. H., & Cryan, J. F. (2005). Differential sensitivity to the motor and hypothermic effects of the GABA B receptor agonist baclofen in various mouse strains. *Psychopharmacology*, *179*(3), 688–699. https://doi.org/10.1007/s00213-004-2086-1

Kaufmann, K., Romaine, I., Days, E., Pascual, C., Malik, A., Yang, L., … Weaver, C. D. (2013). ML297 (VU0456810), the first potent and selective activator of the GIRK potassium channel, displays antiepileptic properties in mice. *ACS Chemical Neuroscience*, *4*(9), 1278–1286. https://doi.org/10.1021/cn400062a

Kilkenny, C., Browne, W., Cuthill, I. C., Emerson, M., & Altman, D. G. (2010). Animal research: Reporting in vivo experiments: The ARRIVE guidelines. *British Journal of Pharmacology*, *160*(7), 1577–1579. https://doi.org/10.1111/j.1476-5381.2010.00872.x

Lecci, A., Borsini, F., Mancinelli, A., D'Aranno, V., Stasi, M. A., Volterra, G., & Meli, A. (1990). Effect of serotoninergic drugs on stress-induced hyperthermia (SIH) in mice. *Journal of Neural Transmission. General Section*, *82*(3), 219–230. https://doi.org/10.1007/BF01272765

Lecci, A., Borsini, F., Volterra, G., & Meli, A. (1990). Pharmacological validation of a novel animal model of anticipatory anxiety in mice. *Psychopharmacology*, *101*(2), 255–261. https://doi.org/10.1007/BF02244136

Lee, S. W., Anderson, A., Guzman, P. A., Nakano, A., Tolkacheva, E. G., & Wickman, K. (2018). Atrial GIRK channels mediate the effects of vagus nerve stimulation on heart rate dynamics and arrhythmogenesis. *Frontiers in Physiology*, *9*, 943. https://doi.org/10.3389/fphys.2018.00943

Lister, R. G. (1990). Ethologically-based animal models of anxiety disorders. *Pharmacology & Therapeutics*, *46*(3), 321–340. https://doi.org/10.1016/0163-7258(90)90021-S

Llamosas, N., Bruzos-Cidon, C., Rodriguez, J. J., Ugedo, L., & Torrecilla, M. (2015). Deletion of GIRK2 subunit of GIRK channels alters the 5-HT_{1A} receptor-mediated signaling and results in a depression-resistant behavior. *The International Journal of Neuropsychopharmacology*, *18*(11), pyv051. https://doi.org/10.1093/ijnp/pyv051

Lujan, R., & Aguado, C. (2015). Localization and targeting of GIRK channels in mammalian central neurons. *International Review of Neurobiology*, *123*, 161–200. https://doi.org/10.1016/bs.irn.2015.05.009

Lujan, R., Marron Fernandez de Velasco, E., Aguado, C., & Wickman, K. (2014). New insights into the therapeutic potential of Girk channels. *Trends in Neurosciences*, *37*(1), 20–29. https://doi.org/10.1016/j.tins.2013.10.006

Luscher, C., Jan, L. Y., Stoffel, M., Malenka, R. C., & Nicoll, R. A. (1997). G protein-coupled inwardly rectifying K^+ channels (GIRKs) mediate postsynaptic but not presynaptic transmitter actions in hippocampal neurons. *Neuron*, *19*(3), 687–695. https://doi.org/10.1016/S0896-6273(00)80381-5

Marron Fernandez de Velasco, E., Zhang, L., Vo, N. B., Tipps, M., Farris, S., Xia, Z., … Wickman, K. (2017). GIRK2 splice variants and neuronal G protein-gated K^+ channels: Implications for channel function and behavior. *Scientific Reports*, *7*(1), 1639. https://doi.org/10.1038/s41598-017-01820-2

Mesirca, P., Bidaud, I., Briec, F., Evain, S., Torrente, A. G., Le Quang, K., … Mangoni, M. E. (2016). G protein-gated IKACh channels as therapeutic targets for treatment of sick sinus syndrome and heart block. *Proceedings of the National Academy of Sciences of the United States of America*, *113*(7), E932–E941. https://doi.org/10.1073/pnas.1517181113

Mesirca, P., Marger, L., Toyoda, F., Rizzetto, R., Audoubert, M., Dubel, S., … Mangoni, M. E. (2013). The G-protein-gated K^+ channel, IKACh, is required for regulation of pacemaker activity and recovery of resting heart rate after sympathetic stimulation. *The Journal of General Physiology*, *142*(2), 113–126. https://doi.org/10.1085/jgp.201310996

Nimitvilai, S., Lopez, M. F., & Woodward, J. J. (2018). Effects of monoamines on the intrinsic excitability of lateral orbitofrontal cortex neurons in alcohol-dependent and non-dependent female mice. *Neuropharmacology*, *137*, 1–12. https://doi.org/10.1016/j.neuropharm.2018.04.019

Ramos-Hunter, S. J., Engers, D. W., Kaufmann, K., Du, Y., Lindsley, C. W., Weaver, C. D., & Sulikowski, G. A. (2013). Discovery and SAR of a novel series of GIRK1/2 and GIRK1/4 activators. *Bioorganic & Medicinal Chemistry Letters*, *23*(18), 5195–5198. https://doi.org/10.1016/j.bmcl.2013.07.002

Raymond, J. R., Mukhin, Y. V., Gettys, T. W., & Garnovskaya, M. N. (1999). The recombinant 5-HT1A receptor: G protein coupling and signalling pathways. *British Journal of Pharmacology*, *127*(8), 1751–1764. https://doi.org/10.1038/sj.bjp.0702723

Rodgers, R. J., Cole, J. C., & Harrison-Phillips, D. J. (1994). "Cohort removal" induces hyperthermia but fails to influence plus-maze behaviour in male mice. *Physiology & Behavior*, *55*(1), 189–192. https://doi.org/10.1016/0031-9384(94)90030-2

Sanchez-Rodriguez, I., Temprano-Carazo, S., Najera, A., Djebari, S., Yajeya, J., Gruart, A., … Navarro-López, J. D. (2017). Activation of G-protein-gated inwardly rectifying potassium (Kir3/GirK) channels rescues hippocampal functions in a mouse model of early amyloid-β pathology. *Scientific Reports*, *7*(1), 14658. https://doi.org/10.1038/s41598-017-15306-8

Selimbeyoglu, A., Kim, C. K., Inoue, M., Lee, S. Y., Hong, A. S. O., Kauvar, I., … Deisseroth, K. (2017). Modulation of prefrontal cortex excitation/inhibition balance rescues social behavior in CNTNAP2-deficient mice. *Science Translational Medicine*, *9*(401), eaah6733. https://doi.org/10.1126/scitranslmed.aah6733

Slesinger, P. A., & Wickman, K. (Eds.) (2015). *Structure to function of G protein-gated inwardly rectifying (GIRK) channels*. *International Review of Neurobiology*. Amsterdam, Netherlands: Elsevier.

Usowicz, M. M., & Garden, C. L. (2012). Increased excitability and altered action potential waveform in cerebellar granule neurons of the Ts65Dn mouse model of Down syndrome. *Brain Research*, *1465*, 10–17. https://doi.org/10.1016/j.brainres.2012.05.027

Vinkers, C. H., van Bogaert, M. J., Klanker, M., Korte, S. M., Oosting, R., Hanania, T., … Groenink, L. (2008). Translational aspects of pharmacological research into anxiety disorders: The stress-induced hyperthermia (SIH) paradigm. *European Journal of Pharmacology*, *585*(2–3), 407–425. https://doi.org/10.1016/j.ejphar.2008.02.097

Vogels, T. P., Sprekeler, H., Zenke, F., Clopath, C., & Gerstner, W. (2011). Inhibitory plasticity balances excitation and inhibition in sensory pathways and memory networks. *Science*, *334*(6062), 1569–1573. https://doi.org/10.1126/science.1211095

Walsh, K. B. (2011). Targeting GIRK channels for the development of new therapeutic agents. *Frontiers in Pharmacology*, *2*, 64.

Wenthur, C. J., Morrison, R., Felts, A. S., Smith, K. A., Engers, J. L., Byers, F. W., … Lindsley, C. W. (2013). Discovery of (*R*)-(2-fluoro-4-((-4-methoxyphenyl)ethynyl)phenyl) (3-hydroxypiperidin-1-yl)methanone (ML337), an $mGlu_3$ selective and CNS penetrant negative allosteric modulator (NAM). *Journal of Medicinal Chemistry*, *56*(12), 5208–5212. https://doi.org/10.1021/jm400439t

Wickman, K., Karschin, C., Karschin, A., Picciotto, M. R., & Clapham, D. E. (2000). Brain localization and behavioral impact of the G-protein-gated K^+ channel subunit GIRK4. *The Journal of Neuroscience*, *20*(15), 5608–5615. https://doi.org/10.1523/JNEUROSCI.20-15-05608.2000

Wickman, K., Nemec, J., Gendler, S. J., & Clapham, D. E. (1998). Abnormal heart rate regulation in GIRK4 knockout mice. *Neuron*, *20*(1), 103–114. https://doi.org/10.1016/S0896-6273(00)80438-9

Wieting, J. M., Vadukoot, A. K., Sharma, S., Abney, K. K., Bridges, T. M., Daniels, J. S., … Hopkins, C. R. (2017). Discovery and characterization of 1*H*-pyrazol-5-yl-2-phenylacetamides as novel, non-urea-containing GIRK1/2 potassium channel activators. *ACS Chemical Neuroscience*, *8*(9), 1873–1879. https://doi.org/10.1021/acschemneuro.7b00217

Wydeven, N., Marron Fernandez de Velasco, E., Du, Y., Benneyworth, M. A., Hearing, M. C., Fischer, R. A., … Wickman, K. (2014). Mechanisms underlying the activation of G-protein-gated inwardly rectifying K^+ (GIRK) channels by the novel anxiolytic drug, ML297. *Proceedings of the National Academy of Sciences of the United States of America*, *111*(29), 10755–10760. https://doi.org/10.1073/pnas.1405190111

Wydeven, N., Posokhova, E., Xia, Z., Martemyanov, K. A., & Wickman, K. (2014). RGS6, but not RGS4, is the dominant regulator of G protein signaling (RGS) modulator of the parasympathetic regulation of mouse heart rate. *The Journal of Biological Chemistry*, *289*(4), 2440–2449. https://doi.org/10.1074/jbc.M113.520742

Wydeven, N., Young, D., Mirkovic, K., & Wickman, K. (2012`). Structural elements in the Girk1 subunit that potentiate G protein-gated potassium channel activity. *Proceedings of the National Academy of Sciences of the United States of America*, *109*(52), 21492–21497. https://doi.org/10.1073/pnas.1212019110

Yu, H. B., Li, M., Wang, W. P., & Wang, X. L. (2016). High throughput screening technologies for ion channels. *Acta Pharmacologica Sinica*, *37*(1), 34–43. https://doi.org/10.1038/aps.2015.108

Zethof, T. J., Van der Heyden, J. A., Tolboom, J. T., & Olivier, B. (1995). Stress-induced hyperthermia as a putative anxiety model. *European Journal of Pharmacology*, *294*(1), 125–135. https://doi.org/10.1016/0014-2999(95)00520-X

Zou, B., Yu, H., Babcock, J. J., Chanda, P., Bader, J. S., McManus, O. B., & Li, M. (2010). Profiling diverse compounds by flux- and electrophysiology-based primary screens for inhibition of human *Ether-à-go-go* related gene potassium channels. *Assay and Drug Development Technologies*, *8*(6), 743–754. https://doi.org/10.1089/adt.2010.0339

SUPPORTING INFORMATION

Additional supporting information may be found online in the Supporting Information section at the end of the article.

How to cite this article: Vo BN, Abney KK, Anderson A, et al. VU0810464, a non-urea G protein-gated inwardly rectifying K^+ ($K_{ir}3$/GIRK) channel activator, exhibits enhanced selectivity for neuronal $K_{ir}3$ channels and reduces stress-induced hyperthermia in mice. *Br J Pharmacol*. 2019;176:2238–2249. https://doi.org/10.1111/bph.14671